2015

Effects of Nanosecond Pulse Electric Fields on Cellular Elasticity

Diganta Dutta
Old Dominion University

Anthony Asmar
Old Dominion University

Michael W. Stacey
Old Dominion University, mstacey@odu.edu

Decrease in cellular elasticity following nanosecond pulsed electric field exposure

*Diganta Dutta[1], *Anthony Asmar[2], Michael Stacey[2]

[1]Institute of Micro & Nanotechnology, Mechanical & Aerospace Engineering Department, Old Dominion University, Norfolk, VA, USA

[2]Frank Reidy Research Center for Bioelectrics, Old Dominion University, Norfolk, VA, USA

*The two authors contributed equally to this work

Corresponding author:

Dr. Michael Stacey, Frank Reidy Research Center for Bioelectrics, 4211 Monarch Way, Norfolk, VA 23508 USA

Email: mstacey@odu.edu

Telephone: 757 683 2245

Fax: 757 451 1010

Abstract

We investigated the effects of a single 60 nanosecond pulsed electric field (nsPEF) of low (15kV/cm) and high (60 kV/cm) field strengths on cellular morphology and membrane elasticity in Jurkat cells using fluorescent microscopy and atomic force microscopy (AFM). We performed force displacement measurements on cells using AFM and calculated the Young's modulus for membrane elasticity. We found that a single nsPEF of low field strength did not induce any apparent cytoskeletal breakdown and had minor morphological changes. Interestingly, force measurements and calculation of Young's modulus showed a significant decrease in cellular elasticity. A 60 kV/cm nsPEF induced disruption of actin, stark morphological changes, and a marked decrease in elasticity. We suggest that the cellular morphology is mainly dependent on stabilization by the actin cytoskeleton, while the elasticity changes are partially dependent on the cytoskeletal integrity.

Keywords: AFM, Young's Modulus, nsPEF, Jurkats, actin cytoskeleton, pulse electric fields.

1. Introduction

The application of electric fields across a biological membrane, causing lipid rearrangements called pores to form, is referred to as electroporation (EP). Depending on the electric field strength, pulse number and duration, the membrane effects can be temporary and will not induce cell death (Neumann and Rosenheck, 1972; Schoenbach et al., 2001). Conventional EP typically consists of pulses with duration greater than 100 μs and sub-kV/cm voltages resulting in the formation of large heterogeneous pores in the plasma membrane (Gabriel and Teissie, 1999; Gowrishankar and Weaver, 2006; Tekle et al., 1990). Cortical actin destabilization was shown to not be related to electropermeabilization of the cell membrane under long pulse durations (Chopinet et al., 2013, 2014; Chopinet et al., 2014).

Nanosecond pulsed electric fields (nsPEFs) are characterized as high voltage (greater than 10 kV/cm), short duration (sub-μs) electrical pulses capable of inducing cellular effects different from conventional EP. NsPEF-related effects includes the creation of dense, homogenous nanopores in the cell plasma membrane and pore formation in intracellular membranes, such as organelles and the nuclear envelope (Schoenbach et al., 2001; Gowrishankar et al., 2006; Pakhomov et al., 2009). NsPEFs permeabilize the cell membrane without the uptake of propidium iodide (Pakhomov et al., 2007), unlike conventional EP, and is associated with an increase of intracellular calcium from both intracellular stores and extracellular sources (White et al., 2004; Semenov et al., 2013). The formation of nanopores and penetration into intracellular structures is attributed to pulse durations shorter than the charging time of the cell membrane (Schoenbach et al., 2001; Pakhomov et al., 2007). The permeabilization of external and internal membranes is thought to be the main mechanism of cell death. Previously, we observed that

nsPEFs are able to induce chromosome and telomere damage and actin cytoskeleton disruption which was found to also contribute to cell death (Stacey et al., 2003; Stacey et al., 2011).

Many investigations have studied the nature of pore formation in cells subjected to nsPEFs while the morphological changes and overall membrane elasticity remain relatively unknown. In this study, we utilized atomic force microscopy (AFM) and fluorescent microscopy to determine the changes in cellular morphology and elasticity.

2. Methods

2.1 Cell Culture

Jurkat cells are an immortalized human T-lymphocyte cell line which grow in suspension. Jurkat clone E6-1 (ATCC, Manassas, VA, USA) were cultured in RPMI 1640 medium (Atlanta Biologicals, Norcross, GA, USA) supplemented with 10% fetal bovine serum (Atlanta Biologicals), 2 mM L-glutamine (Gibco/Invitrogen, Carlsbad, CA, USA), 50 IU/ml penicillin (Gibco/Invitrogen), and 50 mg/ml streptomycin (Gibco/Invitrogen) at 37°C with 5% CO_2 in air.

2.2 Cell Electroporation and Preparation

Cells were placed in cuvettes with 1 mm gaps (BioSmith, San Clemente, CA, USA) and exposed to a single pulse of 60 nanosconds with pulse strengths of 0, 15, and 60 kV/cm. The pulses were generated using the equipment previously described (Schoenbach et al., 2001). After exposure, cells were immediately fixed with 4% paraformaldehyde then transferred to poly-L-lysine coated coverslips (Sigma-Aldrich, St. Louis, MO, USA). After fixation, cells were washed in PBS and then imaged using atomic force microscopy or the cytoskeleton stained with Oregon

green 488 phalloidin (Invitrogen) and the nuclei counterstained with DAPI (Sigma). Electronic fluorescent images were captured using an Olympus DP70 CCD camera through an Olympus BX51 microscope (Olympus America Inc., Center Valley, PA, USA).

2.3 Atomic Force Microscopy

The height, phase, and NSOM images of the Jurkat cells were obtained by using a Multiview-4000 multi-probe atomic force microscope (Nanonics Imaging, Jerusalem, ISR) as previously described (Stacey et al., 2013). In brief, the coverslips with fixed cells were loaded onto the AFM stage and images with a resolution of 256 x 256 pixels were obtained using NWS (Nanonics) and WSxM 5.0 (Nanotech Electronica, Madrid, ESP) software with a 20 nm parabolic quartz tip in tapping mode. The cantilever has a spring constant of 2600 µN/µm and resonance frequency of 33.97 kHz. Calibration was performed using a silicon grid and a profilometer. Force measurements were processed and verified using silicon and polydimethylsiloxane (PDMS).

2.4 Young's Modulus

To calculate the Young's modulus, a modified Hertz model known as the Derjaguin-Muller-Toporov (DMT) model was used (Derjaguin et al., 1975). The DMT model gives the stress distribution with an indentation depth δ in the area of contact using the equation below:

(1) $F_{tip} = \frac{4}{3} E^* \delta^{\frac{3}{2}} \sqrt{R} + F_{adh}$

The applied load using a parabolic tip is F_{tip} where the apical radius is R, the indentation depth is δ, and E^* is the relative Young's modulus. The DMT model differs from the Hertz model in that it also factors for the adhesion force (F_{adh}) of two elastic bodies caused by intermolecular

forces. The Young's modulus was calculated and graphed using MATLAB (MathWorks, Natick, MA, USA). The calculated elasticity was calibrated using PDMS as a standard. Statistical analysis was performed using Student's *t*-test and $p < 0.05$ indicated a significant result.

3. Results

3.1 Actin and Morphology

The application of nsPEFs to cells is known to cause the formation of nanopores. Computational modeling and experimental studies have studied the size, density, and lifespan of these pores (Gowrishankar and Weaver, 2006; Pakhomov et al., 2009; Pakhomov et al., 2007; Vasilkoski et al., 2006). The effect of these high energy, low duration electric fields on the membrane integrity and cytoskeleton is not well known. We investigated the cellular cytoskeleton with fluorescent microscopy. Using DAPI and Phalloidin, we were able to visualize the nucleus and actin cytoskeleton (Figure 1). Jurkat cells are suspension cells which have a round cell morphology. Untreated cells (0 kV/cm) display a nucleus with a relatively round, crisp cytoskeletal outline (Figure 1A-C). Following the application of a 15 kV/cm nsPEF, the actin cytoskeleton appears to be intact and appears similar to the untreated cells (Figure 1D-F). A 60 kV/cm nsPEF caused the actin cytoskeleton at the periphery of the cell to become more diffuse and some cells also lost their round shape (Figure 1G-I). The diffuse localization of actin and formation of foci suggests that the 60 kV/cm nsPEF induced major destabilization of the actin cytoskeleton.

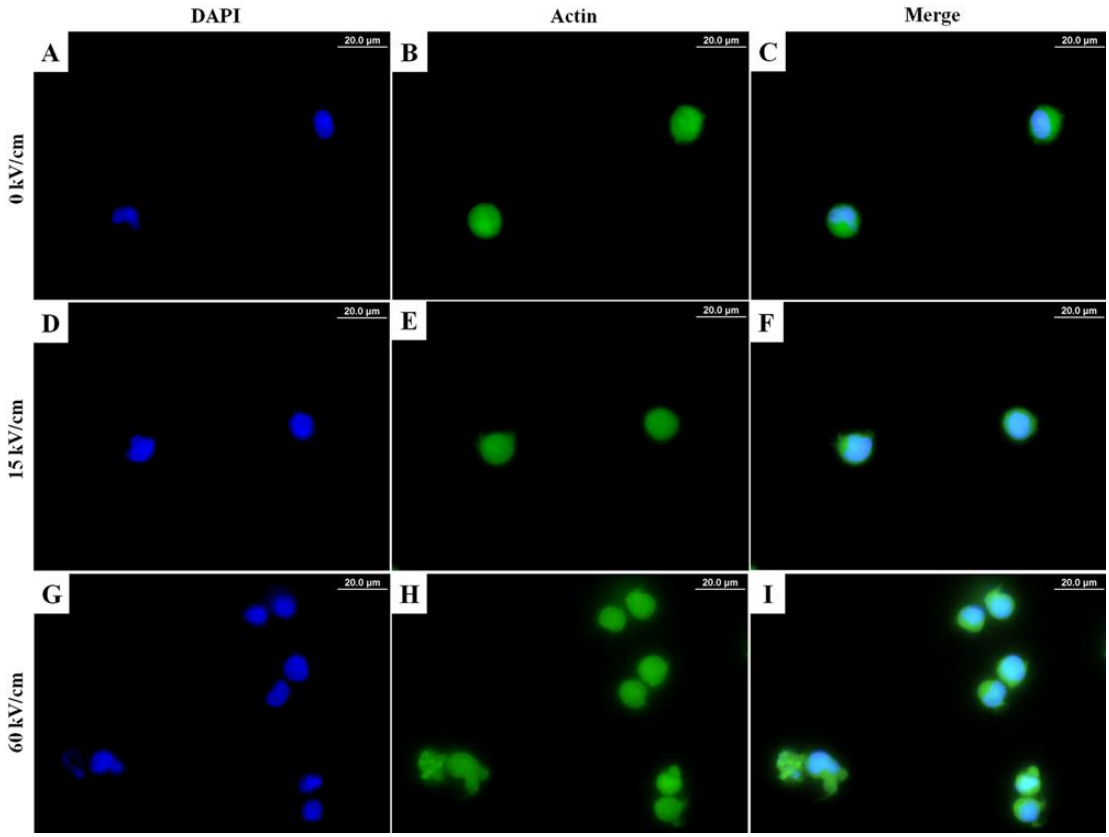

Figure 1. Actin analysis of cells exposed to nanosecond pulsed electric fields (nsPEF) using fluorescent microscopy. DAPI (blue) staining of nucleic acids, Phalloidin (green) staining of F-actin, and merged images of Jurkat cells exposed to a single 60 ns pulse of (**A**-**C**) 0 kV/cm, (**D**-**F**) 15 kV/cm and (**F**-**I**) 60 kV/cm.

3.2 AFM and Morphology

Using AFM and NSOM, the morphological changes associated with the application of different nsPEFs were visualized (Figure 2). The AFM data collected was used to produce the height and phase profiles. The height profile (Figure 2A-C) is representative of changes in topography from the physical interaction with the surface, while the phase profile is dependent on the height, hardness, and chemical makeup of the surface (Figure 2D-F). NSOM was used to visualize the morphology optically (Figure 2G-I). Using the AFM data collected, three-

dimensional representations were also generated (Figure 2J-L). We found that a single 60 ns, 15 kV/cm pulse induced a small change in the morphology by changing the cell from a rounded (Figure 2J) to an oval shape (Figure 1K). The 60 kV/cm nsPEF had deleterious effects showing marked morphological changes (Figure 1L).

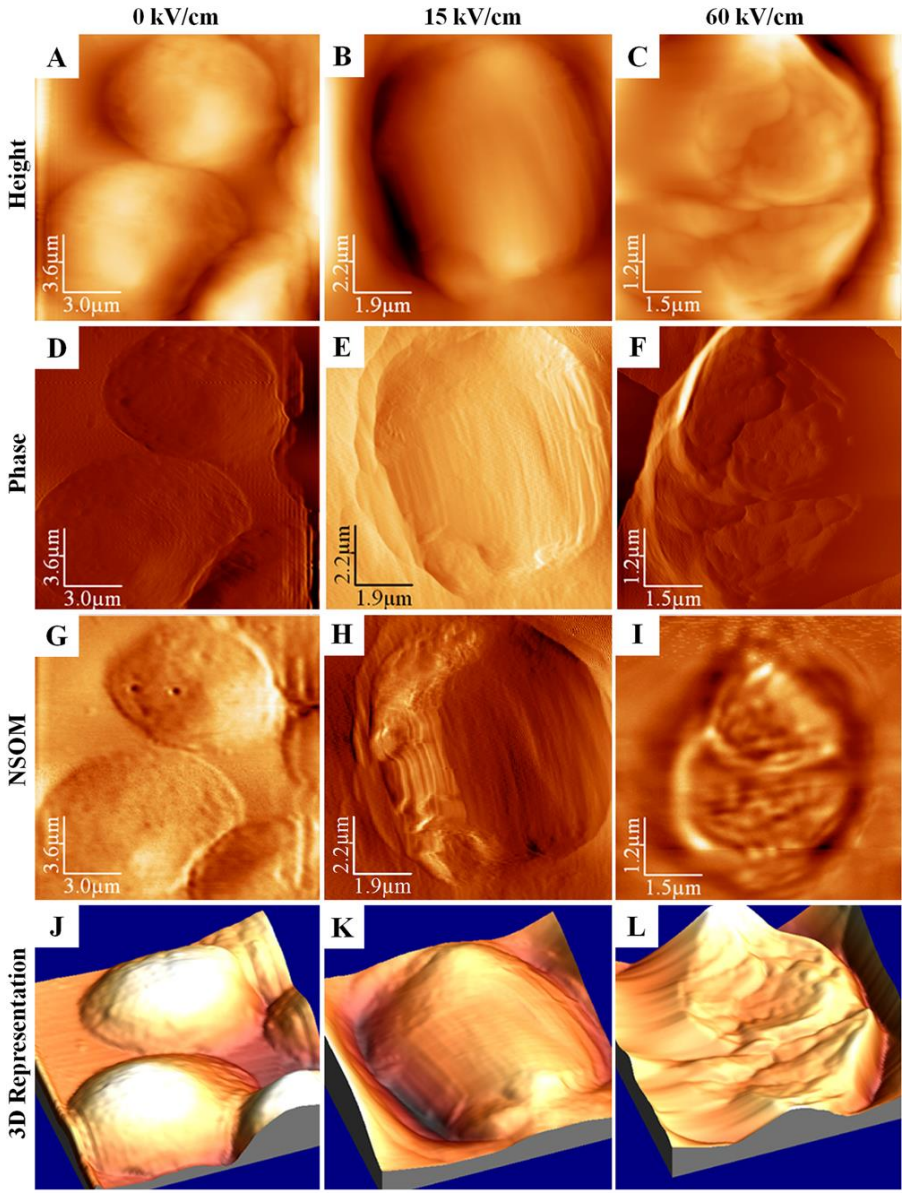

Figure 2. Atomic force microscopy (AFM) and near-field scanning optical microscopy (NSOM) of Jurkat cells exposed to nanosecond pulsed electric fields (nsPEFs). (**A-C**) AFM height images of cells exposed to 0, 15, and 60 kV/cm nsPEFs, respectively. (**D-F**) NSOM images of Jurkat

cells exposed to 0, 15, and 60 kV/cm nsPEFs, respectively. (**G-I)** AFM phase images of Jurkat cells exposed to 0, 15, and 60 kV/cm nsPEFs, respectively. (**J-L**) Three-dimensional representations based on AFM height measurements of Jurkat cells exposed to 0, 15, and 60 kV/cm nsPEFs, respectively.

3.3 Young's Modulus

Using force spectroscopy mode atomic force microscopy, force-indentation measurements were taken and used to calculate the Young's modulus. The Young's modulus was calibrated with known values for PDMS. Our force-indentation measurements and calculated Young's modulus for PDMS was 550.33 (±15.70) kPa (Figure 3), which is in agreement with the previously published value of 549 kPa (Armani et al., 1999). Measurement of the elasticity of the cells (Figure 4) found a 53% decrease in the Young's modulus when Jurkat cells were exposed to 15 kV/cm (Figure 4E and Table 1). No apparent observed change to the actin cytoskeleton network under fluorescence microscopy suggests that the reduction in Young's modulus is due to factors other than the cytoskeleton, possibly the porosity of the cell membrane. However, the application of a 60 kV/cm nsPEF resulted in an 85% decrease of the Young's modulus at the maximum indentation depth when compared to 0 kV/cm (Figure 4E and Table 1). Taken together the changes observed to the actin cytoskeleton in Figure 1H, and given that the cytoskeleton network confers shape, rigidity, and elasticity to the cells, then the decreased Young's modulus with increasing electric field strengths suggests that nsPEFs disrupt the cytoskeleton resulting in decreased stiffness of the cell membrane.

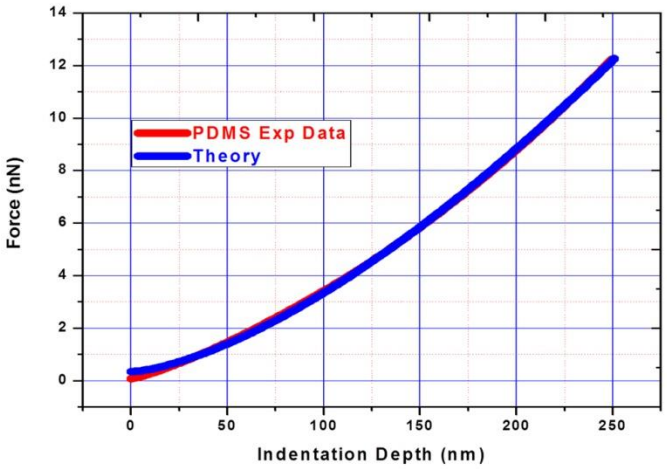

Figure 3. Force-indentation measurements of PDMS using force spectroscopy mode atomic force microscopy.

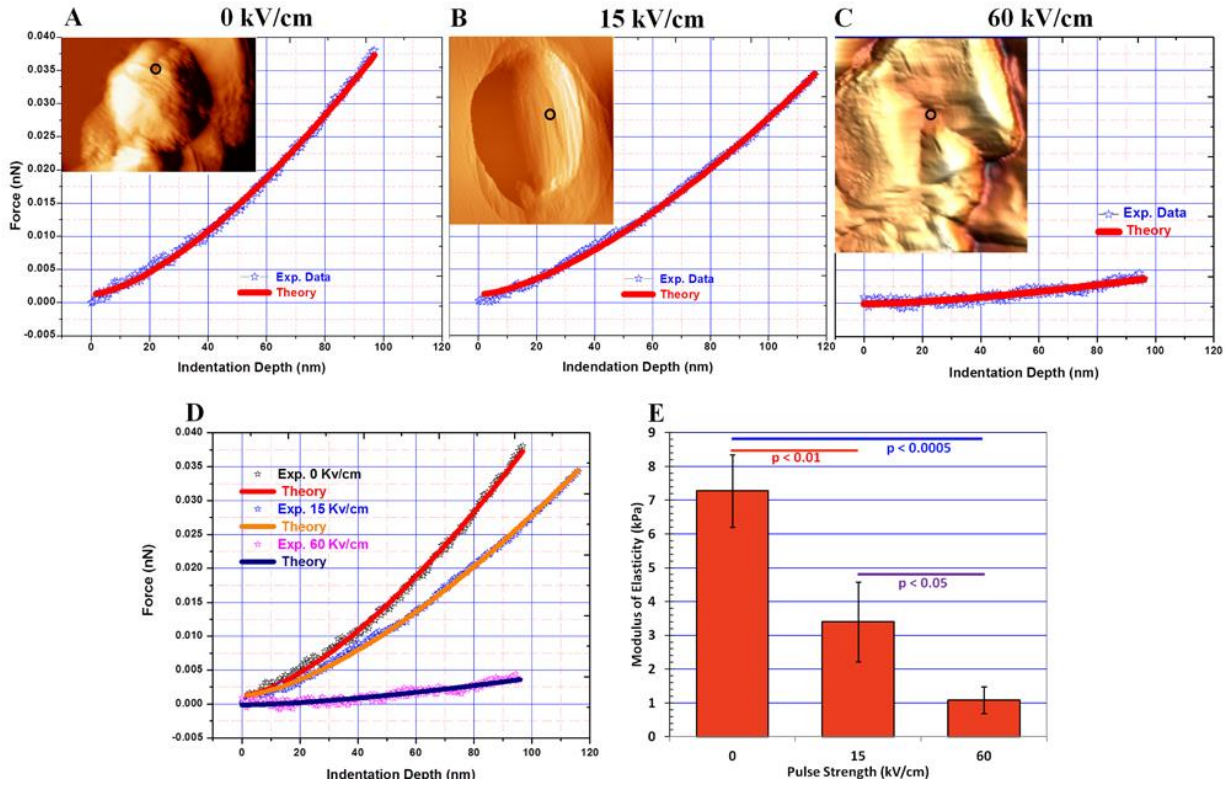

Figure 4. Young's modulus of Jurkat cells exposed to nanosecond pulsed electric fields (nsPEFs) using force spectroscopy mode atomic force microscopy (FS-AFM). Membrane force-indentation measurements of cells exposed to (**A**) 0, (**B**) 15, and (**C**) 60 kV/cm nsPEFs using FS-AFM. The black circles mark the point on the cell where force measurements were taken.

Comparison of (**D**) force-indentation measurements and (**E**) Young's modulus in cells pulsed for 60 ns at 0, 15, and 60 kV/cm (n = 3 for all conditions).

Table 1. Calculated Young's Modulus

Pulse Strength	0 kV/cm	15 kV/cm	60 kV/cm
Mean (±SD)	7.27 (±1.07)	3.40 (±1.19)	1.09 (±0.395)
% Reduction from 0 kV/cm	---	53.3%**	85.0%***

Calculated Young's Modulus given in kPa.
** Statistically significant ($p < 0.01$)
*** Statistically significant ($p < 0.001$)

4. Discussion

This is the first study measuring nanosecond pulsed electric field effects on membrane elasticity. We investigated the changes in the cellular morphology and elasticity of Jurkat cells due to a single 60 nanosecond pulsed electric field (nsPEF) of low (15kV/cm) and high (60 kV/cm) field strengths using fluorescent microscopy and atomic force microscopy (AFM). Fluorescent staining with phalloidin was used to visualize the filamentous actin and DAPI for nucleic acids. We performed force-indentation measurements on cells using AFM and calculated the Young's modulus by fitting our force-indentation measurements into a modified Hertz model known as the Derjaguin-Muller-Toporov (DMT) model. The Young's modulus is used to characterize the elastic modulus, or stiffness, of the cell membrane which is the ability to resist deformation. We also imaged the cellular morphology using near-field scanning optical microscopy complemented by AFM height and phase imaging.

The Jurkat cell line was chosen due to their growth in suspension with a round morphology, allowing for easier observation of morphological changes. Following a low field

strength nsPEF application to Jurkats, the cells became more oval in shape (Figure 2K). Though phalloidin staining did not show any distinct changes in the actin cytoskeleton (Figure 1E), the elasticity was significantly reduced by 53% (Figure 3E). This suggests that the low field strength nsPEF has a considerable effect on the cell membrane but not the actin cytoskeleton, in agreement with low field strengths experienced under long pulsing conditions (Chopinet et al., 2013; Chopinet et al., 2014). The elasticity decrease seems to be independent of actin effects and likely due to lipid rearrangements. The high nsPEF strength caused substantial changes in cell morphology (Figure 2L), disruption of the actin cytoskeleton (Figure 1H), and an 85% reduction in elasticity (Figure 3E). The depolymerization and disruption of actin filaments, possible destruction of the cell cortex (Berghofer et al., 2009), and lipid rearrangements when using high field strengths are likely tied to the extensive morphological and elasticity changes.

5. Conclusion

In conclusion, our results show that nanosecond pulsed electric fields induce substantial changes in the cell elasticity. Specifically, we observed significant decreases in the membrane elasticity using both low and high field strengths, while actin destabilization was apparent with a high field strength. The observed effects are likely caused by long-lasting permeabilization of the membrane as the measurements were performed on cells that were fixed less than one minute of the application of the nsPEF. These long-lasting and even irreversible effects are partially dependent on the cell cytoskeleton. The plasma membrane interacts and is stabilized by the cell cytoskeleton (Berghofer et al., 2009). The destabilization of the actin cytoskeleton would result in further loss of membrane integrity and aberrant cellular morphology which was observed using nsPEFs with a high field strength (60kC/cm, Figure 1H and 2L). This is supported by our

previous findings where disruption of actin before the application of nsPEFs resulted in a significant decrease in the survival of cells (Stacey et al., 2011). Using AFM, we were able to visualize and determine the level of membrane destabilization using force-indentation measurements. In the future, we intend to investigate the degree of stabilization that the actin cytoskeleton contributes to the plasma membrane when applying nsPEFs. The diverse effects of electric fields in biological systems is important, and nsPEFs provide a tool for extending the scope of these investigations as they predominantly affect internal cell structures compared to long pulse conditions.

Acknowledgements

Research reported in this publication was supported by the National Institute of Arthritis and Musculoskeletal and Skin Diseases of the National Institute of Health under the award number R21AR063334. We also acknowledge the Department of Biological Sciences, Old Dominion University, Norfolk, VA.

References

1 Neumann, E. & Rosenheck, K. Permeability changes induced by electric impulses in vesicular membranes. *The Journal of membrane biology* **10**, 279-290, (1972).

2 Schoenbach, K. H., Beebe, S. J. & Buescher, E. S. Intracellular effect of ultrashort electrical pulses. *Bioelectromagnetics* **22**, 440-448, (2001).

3 Gabriel, B. & Teissie, J. Time courses of mammalian cell electropermeabilization observed by millisecond imaging of membrane property changes during the pulse. *Biophys J* **76**, 2158-2165, (1999). doi:10.1016/S0006-3495(99)77370-4

4 Gowrishankar, T. R. & Weaver, J. C. Electrical behavior and pore accumulation in a multicellular model for conventional and supra-electroporation. *Biochem Biophys Res Commun* **349**, 643-653, (2006). doi:10.1016/j.bbrc.2006.08.097

5 Tekle, E., Astumian, R. D. & Chock, P. B. Electro-permeabilization of cell membranes: effect of the resting membrane potential. *Biochem Biophys Res Commun* **172**, 282-287, (1990).

6 Chopinet, L., Roduit, C., Rols, M. P. & Dague, E. Destabilization induced by electropermeabilization analyzed by atomic force microscopy. *Biochim Biophys Acta* **1828**, 2223-2229, (2013). doi:10.1016/j.bbamem.2013.05.035

7 Chopinet, L., Dague, E. & Rols, M. P. AFM sensing cortical actin cytoskeleton destabilization during plasma membrane electropermeabilization. *Cytoskeleton* **71**, 587-594, (2014). doi:10.1002/cm.21194

8 Gowrishankar, T. R., Esser, A. T., Vasilkoski, Z., Smith, K. C. & Weaver, J. C. Microdosimetry for conventional and supra-electroporation in cells with organelles. *Biochem Biophys Res Commun* **341**, 1266-1276, (2006). doi:10.1016/j.bbrc.2006.01.094

9 Pakhomov, A. G. *et al.* Lipid nanopores can form a stable, ion channel-like conduction pathway in cell membrane. *Biochem Biophys Res Commun* **385**, 181-186, (2009). doi:10.1016/j.bbrc.2009.05.035

10 Pakhomov, A. G. *et al.* Long-lasting plasma membrane permeabilization in mammalian cells by nanosecond pulsed electric field (nsPEF). *Bioelectromagnetics* **28**, 655-663, (2007). doi:10.1002/bem.20354

11 White, J. A., Blackmore, P. F., Schoenbach, K. H. & Beebe, S. J. Stimulation of capacitative calcium entry in HL-60 cells by nanosecond pulsed electric fields. *J Biol Chem* **279**, 22964-22972, (2004). doi:10.1074/jbc.M311135200

12 Semenov, I., Xiao, S. & Pakhomov, A. G. Primary pathways of intracellular Ca(2+) mobilization by nanosecond pulsed electric field. *Biochim Biophys Acta* **1828**, 981-989, (2013). doi:10.1016/j.bbamem.2012.11.032

13 Pakhomov, A. G. *et al.* Membrane permeabilization and cell damage by ultrashort electric field shocks. *Arch Biochem Biophys* **465**, 109-118, (2007). doi:10.1016/j.abb.2007.05.003

14 Stacey, M. *et al.* Differential effects in cells exposed to ultra-short, high intensity electric fields: cell survival, DNA damage, and cell cycle analysis. *Mutat Res* **542**, 65-75, (2003).

15 Stacey, M., Fox, P., Buescher, S. & Kolb, J. Nanosecond pulsed electric field induced cytoskeleton, nuclear membrane and telomere damage adversely impact cell survival. *Bioelectrochemistry* **82**, 131-134, (2011). doi:10.1016/j.bioelechem.2011.06.002

16 Stacey, M. *et al.* Atomic force microscopy characterization of collagen 'nanostraws' in human costal cartilage. *Micron* **44**, 483-487, (2013). doi:10.1016/j.micron.2012.10.006

17 Derjaguin, B. V., Muller, V. M. & Toporov, Y. P. Effect of Contact Deformations on Adhesion of Particles. *J Colloid Interf Sci* **53**, 314-326, (1975). doi:Doi 10.1016/0021-9797(75)90018-1

18 Vasilkoski, Z., Esser, A. T., Gowrishankar, T. R. & Weaver, J. C. Membrane electroporation: The absolute rate equation and nanosecond time scale pore creation. *Physical review. E, Statistical, nonlinear, and soft matter physics* **74**, 021904, (2006).

19 Armani, D., Liu, C. & Aluru, N. Re-configurable fluid circuits by PDMS elastomer micromachining. *Proc Ieee Micr Elect*, 222-227, (1999).

20 Berghofer, T. *et al.* Nanosecond electric pulses trigger actin responses in plant cells. *Biochem Biophys Res Commun* **387**, 590-595, (2009). doi:10.1016/j.bbrc.2009.07.072